An investigation on parameters affecting the optimization of testosterone enanthate loaded solid nanoparticles for enhanced transdermal delivery

Article (Accepted Version)

An investigation on parameters affecting the optimization of testosterone enanthate loaded solid nanoparticles for enhanced transdermal delivery

Mahgol Tajbakhsh [a], Majid. Saeedi [b,*], Jafar Akbari[b], Katayoun Morteza-Semnani [c], Ali Nokhodchi[d], Akbar Hedayatizadeh-Omran[e]

[a] Pharmaceutical Sciences Research Center, Mazandaran University of Medical Sciences, Sari, Iran; [b] Department of Pharmaceutics, Faculty of Pharmacy, Mazandaran University of Medical Sciences, Sari, Iran; [c] Department of Medicinal Chemistry, Faculty of Pharmacy, Mazandaran University of Medical Sciences, Sari, Iran; [d] Pharmaceutics Research Laboratory, School of Life Sciences, University of Sussex, Brighton, BN1 9QJ, UK; [e] Gastrointestinal Cancer Research Center, Mazandaran University of Medical Sciences, Sari, Iran

*Corresponding authors:

Majid Saeedi (msaeedi@mazums.ac.ir; Telephone: +98-1134484800; Fax: +98- 1133261244)

Ali Nokhodchi (a.nokhodchi@sussex.ac.uk; Tel: +44 1273 872811)

Abstract

The current research aimed to formulate and optimize testosterone enanthate-loaded solid lipid nanoparticles (TE-SLNs) for the enhanced TE transdermal delivery. To this end, TE-SLNs were prepared using ultrasound-assisted emulsification technique and their properties and permeation across the excised rat skin were investigated. Evaluation of lipid type as well as the ratio and contents of surfactant mixtures resulted in a polydispersity index, particle size, drug loading, drug encapsulation efficiency, and zeta potential of 0.317± 0.006, 87.66± 1.52 nm, 21.61± 0.45 %, 44.71± 1.14 % and -23.06± 0.50 mV, respectively. ATR-FTIR spectra of TE-SLNs exhibited the prominent functional groups of TE in the formulations, indicating a well-dispersion of TE in the lipid matrix without any chemical interaction with other components of the formulation. Differential scanning calorimetry (DSC) demonstrated that TE in SLNs is in an amorphous state. Transmission electron microscopy (TEM) confirmed that the prepared TE-SLNs have a stable size and maintained their sphericity. The results of TE permeation across the excised rat skin from SLNs displayed cumulative amounts of 110.61±17.7 μg/cm^2, which is 3.2 fold improvement in TE permeation in comparison with the testosterone enanthate solution in oleic acid ($p< 0.05$). Furthermore, no cellular toxicity was observed for the nanoparticles. The results showed that the prepared TE-SLNs can be applied as the potential carriers for transdermal delivery of testosterone enanthate.

Keywords

Testosterone enanthate, Solid lipid nanoparticles, Zeta potential, Encapsulation efficiency, Permeation, Transdermal delivery.

Introduction

Anabolic steroids are a class of compounds involving any medicine or hormonal substance and have a chemical and pharmacological relation with testosterone enanthate. It also would stimulate tissue growth [1]. The first class of anabolic steroids is testosterone esters such as testosterone enanthate (TE), testosterone cypionate, and testosterone undecanoate. In addition, TE and testosterone cypionate are the injectable forms of testosterone esters. However, TE is absorbed slowly, and the peak serum concentration for this substance is about 72 h after its intramuscular (IM) injection [2]. Some researchers indicated that since IM injection of testosterone esters results in local irritation; therefore, the absorption rate might be affected by the local irritation of the tissue [2, 3]. Nevertheless, different research demonstrated the benefits of TE replacement therapy [4]. A study performed in the field revealed that achieving a physiological TE pattern (circadian rhythm) and physiological levels of metabolites (dihydrotestosterone and estradiol) strictly depends on the administration route [2]. Moreover, studies on the administration routes illustrated that the transdermal approach provides some advantages over the oral route or hypodermic injections. Since testosterone enanthate is largely metabolized in the gastrointestinal (GI) and the liver; hence, the oral route needs a high dose and this can cause more and serious side effects in comparison to the transdermal approach [5]. Thus, it would be beneficial to patients to explore a formulation for TE that can provide a systematic release and increase patient compatibility such as the transdermal delivery route. It has been shown that the transdermal route can offer prolonged drug release and increase patient compliance in comparison with the injection and oral drug delivery methods [6]. Due to having many advantages and fewer drawbacks for transdermal delivery compared to other routes, researchers have been tried to develop a reliable delivery system for candidate drugs [7]; and the research led to the introduction of the first TE transdermal system

as a scrotal patch in the late 1980s [8]. According to some researchers, non-scrotal patches have appeared in the late 1990s, and these patches, due to a low level of 5-α reductase in non-scrotal skin, resulted in physiological dihydrotestosterone serum level [9]. It has also been pointed out by researchers, TE patches have some disadvantages, including skin irritation [10], adhesion problems, limited dosing flexibility, and elevated manufacturing cost [2]. It seems it is possible to overcome these limitations by introducing advanced lipid nanoparticles (NPs), such as solid lipid nanoparticles (SLNs). Besides, NPs can be employed for improving the solubility of poorly soluble drugs [11, 12]. It should be noted that TE, which is the model drug in the present research, is also water-insoluble (<0.5μg/mL) with a log P of 3.58. Thus, researchers stated that loading TE in SLNs could be a strategy for improving its solubility. In this context, they developed SLNs as an option for carrier systems [13] so that these SLNs have been greatly considered as one of the innovative colloidal drug carriers to be topically applied [14]. It is believed that SLNs are able to keep useful features of other popular colloidal carriers. Moreover, they do not suffer from any drawbacks concerning physicochemical storage stability, loading capacity (LC), toxicity, feasibility, target-oriented releasing properties, and production scale [15]. In addition, some researchers referred to the SLNs characteristics that can lead to skin hydration and increase drug absorption [16, 17]. Furthermore, researchers have applied SLNs to enhance the skin/dermal uptake of multiple medicines [18-21], which confirms that SLNs have the capability to be served as a topical delivery system for TE.

Although the impact of surfactants mixture on the efficiency of solid lipid nanoparticles carrier has been recently reported [22, 23], there is no comprehensive study to investigate a simultaneous evaluation of surfactants mixture at different HLBs and beeswax to optimize TE-SLNs formulation

for the enhanced transdermal delivery. The properties, toxicity and permeability studies of the prepared TE-SLNs were also evaluated.

2. Materials and methods

2.1. Materials

Testosterone enanthate was purchased from Caspian Tamin Pharmaceutical Company, (Guilan, Rasht, Iran). Stearic acid (SA), palmitic acid (PA), glycerol monostearate (GMS), oleic acid (OA), and tween 80 and span 80, HPLC grade acetonitrile and absolute ethanol were obtained from Merck, Germany. In addition, beeswax (BW) was purchased from John's laboratory (John's laboratory chemicals: India). A Human power 2 system (human Co., Korea) has been used to treat the distilled water. DMSO and 3-(4,5-dimethylthiazol-2-yl)-2,5-diphenyltetrazolium bromide (MTT) were obtained from Sigma (St. Louis, MO, USA).

2.2. Preparation of TE-SLNs

SLNs formulations have been performed by modification of ultrasound-assisted emulsification methods reported in the literature [24, 25]. Typically, a mixture of beeswax and TE was heated to 75 °C and stirred for 20 min to achieve a homogenous oil phase. Then, a mixture of span 80 and tween 80 as a surfactant mixture was dissolved in double distilled water to obtain a surfactant aqueous phase. Both phases (aqueous and oil phases) were separately heated to 75 ºC. After reaching the required temperature, the aqueous phase was added onto the oil phase drop-wise under the stirring condition to produce an oil-in-water emulsion. Then, a probe sonicator was applied to sonicate the mixture (Bandelin; 3100; Germany, with an amplitude of 20% for 10 minutes). After sonication, the nanoemulsion was maintained in the ice bath for 10 min by stirring at 300 rpm to achieve TE-SLNs.

2.3. Description of the prepared TE-SLNs

2.3.1. Size of the nanoparticle, polydispersity index, and zeta potential evaluation

Dynamic light scattering (DLS) with Nano ZS zetasizer (Malvern Instruments, Worcestershire, UK) was employed to measure the particle size mean diameter, polydispersity index, and zeta potential at 25°C with an angle of 90° [26]. It should be noted that all measurements have been carried out in triplicates.

2.3.2. Evaluation of drug loading (DL) encapsulation efficiency (EE)

2.0 mL of freshly prepared TE-SLNs were subjected to centrifugation at 54957 ×g (Sigma; Germany) for 120 min at 4°C to separate the lipid and aqueous phases. After separation of the loaded TE from dispersion the supernatant was passed through a syringe filter (0.22µm), and the amount of free TE in the supernatant was measured via HPLC (Knauer, Berlin, Germany) consisted of the XDB C18 column (5 µm; 4.6×250 mm; Germany) [27]. The detection limit (DL) and quantification limit (QL) were determined using the standard deviation (SD) and the slope (S) of the calibration curve according to the International Conference on Harmonization (ICH) [28] by 3.3 SD/S and 10 SD/S to DL and QL respectively [29]. The mobile phase was a mixture of acetonitrile/water (90:10, v/v), the flow rate was set up at 1 ml/min and UV detection wavelength was 254 nm. The specified working range with DL value of 0.81 µg/ml and QL value of 2.45 µg/ml, was kept in the concentration range of 1-100 µg/ml. Drug encapsulation efficiency (EE%) and drug loading (DL%) were obtained using Eqs. 1 and 2. [30]

*EE (%)= (Total amount of Drug-Free drug/Total amount of drug) *100 (Eq.1.)*

*DL (%)= (Total amount of Drug-Free drug/Total amount of lipid) *100 (Eq.2.)*

2.3.3. ATR-FTIR spectroscopic analysis

Cary 630 FTIR spectrophotometer (Agilent Technologies Inc., CA, USA) with a diamond ATR (Attenuated Total Reflectance) was used to study the TE–excipient interactions. Then, TE, BW, span 80, tween 80, and their physical mixtures were examined by ATR-FTIR. According to the above procedure, the spectra were recorded by placing a low amount of each homogeneous sample on the slit and the samples were scanned from 400 to 4000 cm^{-1} and 2 cm^{-1} of resolution.

2.3.4. Diff erential scanning calorimetry (DSC)

DSC was used to analyze the thermal behavior of the solid lipid, pure drug, and drug-loaded SLNs. Before the heating process, about 4 mg of the samples were weighed in the hermetic crimped aluminum pan, preserved at 30 °C for thirteen minutes. The samples were heated up to 300 °C at a scanning rate of 20 °C/min under a nitrogen atmosphere. Pyris 6, (Perkin Elmer, USA) was used to evaluate the DSC traces. Indium (melting transition = 429.75 K) was used as the standard to calibrate the DSC.

2.3.5. Powder X-ray diffractometer (PXRD) analyses

D8 Advance X-ray diff ractometer (Bruker-binary V2: Germany) (40k; 30mA) was used to obtain the patterns of the powder X-ray diffraction (XRD) for identifying any alterations in the crystal lattice of the substances in the SLNs. Moreover, analysis of the crystalline properties of TE, BW, and freeze-dried TE-SLNs powder was performed by exposing them to Cu Kα radiation at a wavelength of 1.5406 Å. Then, the samples were scanned from 5.000° to 70.000°, 2Θ at a step size of 0.040° and step time of 1 s [26].

2.3.6. Transmission electron microscopy (TEM)

TEM microscope (Philips CM 120 KV, Amsterdam: The Netherlands) was used to examine the TE-SLNs morphology. To this end, some drops of TE-SLNs was placed on carbon-coated copper grids. Then, a 2% (v/v) phosphotungstic acid solution was prepared to negatively stain the nanoparticles for 30 seconds. Finally, the solvent has been let to be dried overnight at room temperature, and TEM visualization has been administered [31].

2.4. Cell viability assay

The human gingival fibroblast cells (HGF3-PI53) were achieved from the National Cell Bank of Iran (*Pasteur Institute* of Iran; Tehran: Iran) and were seeded (2×10^4 cells/well) in order to grow in a 96-well plate. In addition, blank SLNs and distinct concentrations of TE-SLNs were added to the cells after 24 h. All conditions were adjusted three times. Moreover, the rapid growth and vitality of the cells were measured using 3-(4,5-dimethylthiazol-2-yl)-2, 5-diphenyl tetrazolium bromide (MTT) assay. Furthermore, a reaction was found between the MTT agent and its tetrazolium ring for producing blue formazan crystals in the viable cells. After passing 24 and 48 hours, the supernatant was eliminated from each well. Then, phosphate-buffered saline (PBS) was used to wash each cell 3 times for removing nonviable cells. Afterwards, 100 µL of fresh media with 0.5 mg/mL of MTT solution was added into the wells. Then, incubation of the cells was done at 37 °C for four hours in order to form the formazan crystal. Consequently, the supernatant was discarded after incubation. Next, 200 µL of dimethyl sulfoxide was added into the wells to dissolve formazan crystals under continuous pipetting. In addition, a microplate reader (Awareness, USA) was used to measure optical density through the spectrophotometric method at a wavelength of 570 nm. Finally, Eq. 2 was employed to calculate the living cells percentage:

% Cell survival= Sample absorbance – Blank absorbance/Control absorbance- Blank absorbance (Eq.2.)

According to the results, the blank had only the media while the control had the cells with media. It should be noted that the cells with no TE-SLNs were employed as a reference for 100% cell survival. However, the average of the results from 3 different experiments was achieved, and the t-test and Spearman's correlation coefficient were used to do statistical analyses. Finally, a p-value of <0.05 was regarded as statistically significant [32].

2.5. *In-vitro* examination of the skin permeation

This research was designed according to the Ethical Guidelines for Investigations in Laboratory Animals. The Ethics Review Committee for Animal Experimentation of Mazandaran University of Medical Sciences with the ethical code of IR.MAZUMS.REC.96.2975 confirmed the research. Moreover, *in vitro* skin absorption assessment was conducted on the Franz diffusion cell with an efficient diffusion area of 3.8 cm^2. For this purpose, the abdominal area of the male Wistar rats (with a weigh of 120–150g) was shaved. Then, the rats were anaesthetized with 13 mg xylazine/kg and87 mg ketamine/kg of body weight. After 48 h, the rats were sacrificed with chloroform inhalation. Afterwards, abdominal skins were removed by surgery. Next, the skin was precisely cleaned from the adhered sub-cutaneous fats, and placed in a normal saline solution for 24 hours before diff usion experiments. The skins were incised into circular segments and inserted in a Franz diffusion cell between receptor and donor compartments in a way that the stratum corneum side was faced with the donor chamber and the dermal side was faced with the receptor chamber. The receptor section had 70% v/v absolute alcohol/water at 32 °C as a suitable solvent system [33]. Then, 4 mL of nanoemulsion formulation or control formulation was added into the donor section. After adding the nanoemulsion, the donor section was enveloped with parafilm in order to prevent

water evaporation. After 2, 4, 6, 8, 10, 12, and 24 h, the samples were taken and replaced with absolute ethanol/water (70:30). Then, the samples were analyzed with HPLC method. Afterwards, the skins were removed, and deionized water was used to wash them three times followed by drying the samples to measure the sedimented TE in the skin. The removed skins were incised into small pieces and transferred to water tubes where they were soaked for 24h, then they were sonicated for an hour using a bath sonicator. It should be noted that for TE evaluation, the supernatants were filtered by a filter paper, passed another time, filtrated through a syringe filter (0.22 μm), and subsequently, HPLC was used to quantify the samples [26, 34].

2.6. Statistical analysis

All data were analyzed with SPSS2021 and GraphPad Prism 5.0 (version 8.0.0.0; GraphPad Software. Inc., San Diego, California, USA) software. The data were expressed as Mean± SD. Moreover, significant differences between two and more groups were analyzed via Student's t-test and ANOVA, respectively. In addition, P greater than 0.05 was regarded as a statistically significant value in all cases.

3. Results and discussion

3.1. Optimizing TE-SLNs

In the present research, TE-SLNs have been procured via homogenization using the ultrasonic process. All these emulsion systems contained water, lipid, TE, and surfactant or surfactants mixture. It has been found that the relation between interfacial characteristics and emulsion stability is important for the development of a product with high stability [35]. Therefore, surfactants could stabilize emulsions by decreasing interfacial tension and creating mechanical or

electrical obstacles [36, 37]. Moreover, the use of surfactants mixture would not only improve the stability of solid lipid nanoparticles structure and particles amorphous but also reduce their particle size due to its synergy [38, 39]. According to some studies, efficient hydrophilic-lipophilic balance (HLB) value is one of the most effective parameters for an appropriate surfactant system. Thus, the surfactants chemical structure and characteristics should be considered [40-42]. Notably, many nonionic surfactants such as sorbitan fatty acid esters (spans) and the polyoxyethylene sorbitan fatty acid esters (tweens) have found potential pharmaceutical applications [43].

To achieve a stable drug-loaded SLNs, in the current research, binary mixtures of span 80 (HLB: 4.3): tween 80 (HLB: 15) at different amounts (1 to 3 g) and ratios (2:1, 1:1, 1:2, and 0:1) were used to obtain different HLB values (7.8, 9.6, 11.4, and 15, respectively) [23]. Various surfactant mixtures (based on the above-mentioned HLBs) with different lipids such as stearic acid, palmitic acid, glyceryl monostearate, and beeswax have been investigated while the amount of TE has been kept constant. Moreover, suitable solid lipid has been selected based on the stability and nanoparticles characteristics such as polydispersity index, size of the nanoparticles, and zeta potential parameters (data are not shown) [44]. The results showed that TE-SLNs containing SA and PA are not stable. However, the main reason for the instability of the structure of the nanoparticle in both low and high concentrations of lipids and constant amount of surfactants (in every HLB) could be related to the aggregation of particles which was evident from the appearance of the samples. On the other hand, the high chain length of stearic acid and palmitic acid could be another restraint for setting stable TE-SLNs [45]. It has been also found that GMS and BW lipids led to better results, but TE-SLNs instability and PDI have been higher in GMS-containing SLNs compared to the BW-based lipid nanoparticles. Therefore, among various lipids (glycerol monostearate, stearic acid, beeswax, and palmitic acid) that were used as a lipid phase, due to the

267 higher solubility of TE in beeswax, it was selected for further examinations. The results revealed
268 that more than 1 g of BW caused physical instability such as creaming, coalescence, phase
269 separation, and precipitation of SLNs. The results for the surfactant system showed that the optimal
270 values of surfactant mixtures ≤ 3 g led to a transparent dispersion while higher amounts of
271 surfactants made the dispersion opaque, which could be due to the particles aggregation.
272
273 **3.2. Physical properties of TE-SLNs**
274 **3.2.1 The effect of surfactants mixture contents on TE-SLNs properties**
275 According to the studies, the selection of proper amounts of surfactants has a major effect on the
276 quality of the SLN dispersion [15]. Other studies also demonstrated that span 80 is an inexpensive
277 and molecularly heterogeneous mixture of mono-, di-, tri-, and tetra esters with primary diesters
278 and oleoyl (cis-9octadecenoyl) chains [46, 47]. Tween 80 is oleic acid esterified with
279 polyethoxylated sorbitan, with 20 subunits of ethylene oxide in each molecule which made it
280 hydrophilic [48]. The mixtures of these nonionic surfactants with different quantities (1, 2 and 3
281 g) have been used to prepare solid lipid nanoparticles. Based on the results in Table 1 (F1 to F12),
282 it could be concluded that the amounts of surfactants mixture significantly affected the SLNs
283 properties such as the mean particle size, polydispersity index, zeta potential, and EE parameters.
284 In addition, some researchers indicated that different contents of surfactant mixtures (composing
285 of HLBs of 7.8, 9.6, 11.4, and 15) have been screened, while the amounts of TE and BW have
286 been kept constant. Furthermore, the characteristics of the nanoparticles for the investigated
287 formulations indicated that the SLNs containing the least amount of surfactants mixture (1 g) have
288 poor stability (F1, F4, F7, F10, and PDI> 0.5) with a high creaming rate [49]. Nonetheless, other
289 studies revealed that higher quantities of surfactants mixture reduced the surface tension and

290 increased unification of particles during homogenization which could be caused by a significant
291 increase in the surface area [15, 50].
292 It was also found that increasing the quantity of surfactants mixture from 1 g (F1, F4, F7, and F10)
293 to 2 g (F2, F5, F8, and F11) or 3 g (F3, F6, F9, and F12) in all HLBs significantly reduced the
294 mean particle size and polydispersity index, while the zeta potential increased ($P<0.0001$) and
295 resulted in better TE-SLNs stability. As it could be predicted, increasing the surfactant
296 concentration leads to lower the surface tension, and makes the partition of particles easier
297 throughout the preparation [15, 39] and reduces the particle size. Additionally, further steric
298 stabilization of particles can be provided by tween 80 and span 80. The interpenetration of existing
299 long polyethylene chains in the mixture of surfactants restricts the particle freedom and inhibits
300 them from connecting to each other [15]. As reported in the previous study [51], the type of lipid
301 directly affects the zeta potential outcomes. The high zeta potential and stability of the selected
302 formulations could confirm that BW is an appropriate lipid in this research. Further scrutiny of the
303 data in Table 1 demonstrates that increasing the amount of the surfactants mixture from 2 g (F2,
304 F5, F8, and F11) to 3 g (F3, F6, F9, and F12) in all HLBs does not make any significant difference
305 in the SLNs properties, including zeta potential, the mean particle size, and polydispersity index
306 ($P> 0.05$); however, TE encapsulation efficiency significantly decreased ($P<0.0001$). This could
307 be attributed to the enhanced solubility of TE in the aqueous phase with the increase in the amount
308 of the surfactants mixture [52, 53]. According to these results, the optimum amount of surfactants
309 mixture has been found to be 2 g in all different HLBs with constant amounts of TE (0.5 g) and
310 BW (1 g).

311

312 **3.2.2 The effect of HLBs of surfactants mixture on the TE-SLNs properties**

As stated by researchers, the impact of HLBs on the polydispersity index, the mean size of the TE-SLNs particles, zeta potential, and EE can be evaluated by comparing formulations with constant amounts of TE (0.5 g), BW (1 g), and surfactants mixtures (2 g, different compositions of span 80 and tween 80) shown in Table 1 (F2, F5, F8, and F11). Findings revealed that the ratio of span 80/tween 80 >1 gives the highest average particle size (342.66± 0.57 nm) and PDI (0.649± 0.046) as well as the least zeta potential (-10.83±1.10 mV) and encapsulated TE (1.95± 0.36). These observations could be as a result of the particle agglomeration and difference between HLBs of F2 (HLB 7.8) and BW (HLB 12). Moreover, the ratios of span 80/tween 80 ≤ 1 led to a significant decrease in the particle size and PDI, and an increase in the zeta potential and EE % (comparing F2 with F5, F8, and F11). However, using the tween 80 alone as an emulsifier (F11) was not adequate for stabilizing TE-SLNs and gave relatively low EE value (19.17± 1.54 %), average particle size (124.33± 2.51 nm), PDI (0.463± 0.008) and zeta potential (-18.5± 2.3 mV). These results could be related to the HLB value of tween 80, which is not suitable for emulsifying BW with an HLB value of 12. However, a combination of span 80: tween 80 with the ratio of 1:2 and HLB of 11.4 (F8) led to the reduction of the particle size (87.66± 1.52 nm), PDI (0.317± 0.006), and an increase of the zeta potential (-23.06± 0.50 mV) and EE (44.71± 1.14 %). Again, such a condition could be attributed to the HLB values of surfactants mixtures (HLB 11.4) and BW (HLB 12), which are very close values, and result in the TE-SLNs appropriate properties. It should be noted that structural differences between span 80 and tween 80; that is, the lipophilicity of span 80 and hydrophilicity of tween 80 provided the necessary stabilization in the emulsion system, and generated low particle size and PDI as well as high zeta potential and encapsulation efficiency [43]. In addition, researchers confirmed the stability of formulation F8 by measuring the particle size after 90 days of preparation at 4 ˚C and 25 ˚C that showed no significant changes in the average

size of TE-SLNs (data are not shown). According to the study conducted in the field, since it is known that the absolute large value of zeta potential is required for dispersion stability [54], the range of zeta potential measured for SLNs with span 80: tween 80 mixture is not high enough to generate the electrical field around the particles. This could suggest that steric and electrostatic stabilization can prevent the aggregation of nanoparticles [39].

As the maximum encapsulation efficiency (44.71± 1.14 %) has been acquired for F8, all the characterization studies have been conducted for this formulation.

3.2.1. ATR-FTIR analysis

The ATR-FTIR technique has been used to explore the probable physicochemical interaction among the chemicals used to generate SLNs. Fig.1 shows the ATR-FTIR spectra of beeswax, span 80, tween 80, TE, and TE-SLNs. The ATR-FTIR spectra of beeswax [55], span 80 [56], and tween 80 [57] have been compatible with their structures. The TE spectrum exhibited characteristic bands consistent with the published data [58]. Moreover, the characteristic peaks of testosterone enanthate could be observed in the ATR-FTIR spectrum of TE-SLNs. The absorption peaks of ketone C = O stretching, ester C = O stretching and conjugated C = C stretching at respectively about 1674 cm^{-1}, 1730 cm^{-1}, and 1611 cm^{-1} in TE could be detected in the spectrum of TE-SLNs, indicating the successful encapsulation of TE in the SLNs structure. It is also worth to mention that these absorption peaks in the spectrum of TE-SLNs have not been shifted significantly, which indicates the compatibility of the TE-SLNs components. However, there has been no significant interaction between them. In other words, the samples have been actually compatible. The main peaks of each component in the formulation of TE-SLNs are as follows: BW: 2916 cm^{-1} (-CH_2-, asymmetric stretching), 2849 cm^{-1} (-CH_2-, symmetric stretching), 1738 cm^{-1} (C = O, stretching), 1466 cm^{-1} (-CH_2-, bending), and 1167 cm^{-1} (C-O, stretching). Span 80: 3397 cm^{-1} (O-H,

stretching), 2920 cm^{-1} (-CH_2-, asymmetric stretching), 2857 cm^{-1} (-CH_2-, symmetric stretching), 1738 cm^{-1} (C=O, stretching). Tween 80: 3494 cm^{-1} (O-H, stretching), 2912 cm^{-1} (-CH_2-, asymmetric stretching), 2857 cm^{-1} (-CH_2-, symmetric stretching), 1738 cm^{-1} (C=O, stretching). TE: 2927 cm^{-1} (-CH_2-, asymmetric stretching), 2857 cm^{-1} (-CH_2-, symmetric stretching), 1730 cm^{1} (ester C=O, stretching), 1674 cm^{-1} (ketone C=O, stretching), 1611 cm^{-1} (conjugated C=C, stretching), 1171 cm^{-1} (C-O, stretching).

3.2.2. Differential scanning calorimetry (DSC)

As defined in the research protocol, the thermal characterization of NPs has been accomplished by DSC analyses to determine modifications in the crystalline state of the elements after medicine encapsulation. Accordingly, Fig. 2 presents the DSC thermograms of TE, BW, and TE-SLNs. According to the results, DSC thermograms of TE and BW experienced endothermic peaks at 39.4 °C and 61 °C respectively, which corresponds to the respective melting point. These values are compatible with the values reported in the literature with a slight difference (37-38 °C for TE) [59] and (61.8 °C for BW) [60]. Thus, it could be concluded that the disappearance of the characteristic endothermic peak of TE near its melting point (39.4 °C) in the TE-SLNs thermogram could be related to either molecular dispersion of TE or the formation of TE-enriched core into the BW matrix. It could also be assumed that TE would be dissolved in an amorphous state in the molten beeswax during loading [61, 62]. Some researchers believe that this may inhibit TE crystallization in the process of nanoparticle preparation [31, 63].

3.2.3. Powder X-ray diffractometer (PXRD) analyses

The crystallite structure of the SLNs has been investigated to analyze the XRD diffraction patterns of TE, TE-SLNs and BW (Fig. 3). The XRD patterns of TE displayed characteristic peaks at 2θ corresponding to 5.33°, 7.14°, 7.97°, 9.68°, 11.26°, 13.75°, 14.81°, 17.43°, 18.48°, and 19.37° [64]. Other studies demonstrated that the pattern of BW exhibited peaks at 2θ: 19.75°, 21.60°, 23.94°, 40.50°, and 53.07° which are consistent with the orthorhombic crystal structure in beeswax [55, 65, 66]. Moreover, the XRD patterns corresponding to the NPs formulation displayed the peaks corresponding to BW (2θ: 19.61°, 21.52°, 23.86°, and 40.26°). In addition, the disappearance of TE peaks and slight broadening of the TE-SLNs patterns indicated that testosterone enanthate in an amorphous state has been molecularly dispersed into the lipid phase [63] that is in agreement with results of DSC studies.

3.2.4. TEM analysis

TEM images of the TE-SLNs revealed that the nanoparticles are approximately in a uniform spherical shape with average sizes of 50 to 100 nm (Fig. 4). As can be seen, no sign of aggregation has been observed in the images so that the particle size has been under 100 nm. This result could be suggested because DLS provides intensity-based hydrodynamic diameters and mean of particle sizes, while TEM works on dry samples under ultra-high vacuum conditions [67]. In other words, the light scattering method actually evaluates the particle hydrodynamic radius that includes both particle size and the associated layers of the solvent on it. Moreover, these kinds of measurements are dynamic and highly dependent on the particle aggregation or dispersion behaviors in the solution [68].

3.3. *In vitro* cell viability study

In order to investigate the safety of the prepared SLNs, different concentrations of TE-SLNs containing 10 to 100 µg/ml of TE have been examined with different amounts of surfactants (ratio of span 80: tween 80, 1:2) on the Human gingival fibroblast cells (HGF3-PI53) for 24 h and 48 h. The results illustrated lower cell viability for the drug-free SLNs compared to the controls ($P<0.05$) (Fig. 5). It should be mentioned that the toxicity observed in the drug-free SLNs could not be related to the nature of the lipids, while it could be dependent on the characteristics of the surfactants [69] or may be related to the controlled release of TE in the culture medium. However, TE-SLNs at various TE concentrations (10, 25, 50, and 100 µg/ml) showed no cytotoxicity toward normal cells, suggesting that the SLNs cytotoxicity loaded with the lipophilic TE is greatly reduced. The lack of toxicity of TE-SLNs at different TE concentrations (with cell viability near 100 %) compared with the drug-free SLNs (with cell viability about 72 %) could be resulted from binding surfactants to the SLNs surface, which led to a reduction in the surfactants cytotoxicity [70]. In other words, if the surfactants are bounded to the SLNs surface, their toxicity reduces compared to when they are free [69].

3.4. *In vitro* percutaneous absorption study

It has been found that *in vitro* permeation study can be used for evaluating the skin permeation abilities of different systems. Thus, this examination was employed to analyze the percutaneous permeation profile of TE-SLNs. As reported in previous studies, water-insoluble compounds may not be able to penetrate into the excised skin and get into the aqueous receptor fluid *in vitro* [33]. However, for testosterone enanthate that is a water-insoluble drug (< 0.5 mg/ml) in a hydroalcoholic mixture (absolute ethanol/water, 70:30) was added into the Franz cell receptor compartment [52]. Since all prepared formulations were in nanosized range, the results indicate that no meaningful difference was found in the amount of TE absorbed when different particle

sizes was used, while studies have shown that encapsulation efficiency is the determining factor in skin absorption. As can be seen in Fig. 6, studies of the testosterone enanthate skin permeation in Y-axis revealed that the mean cumulative TE permeated amounts from the optimized TE-SLNs and TE-oleic acid solution after 24 h are 110.61±17.70 and 34.6±4.57 µg/cm^2, respectively. Also, based on the Z-axis of this figure, the mean cumulative TE permeated percentages from these two formulations were 1.2±0.04 and 0.06±0.008 %, respectively. Thus, the permeation of TE-SLNs was higher than the oily solution of TE in oleic acid ($P< 0.0001$) at each time intervals of detection, indicating the enhanced penetration of TE-SLNs through rat skin. Factors related to enhanced skin permeation by TE-SLNs are assumed to include, the solubility of the drug, small particle size, large surface area, occlusive effect and presence of permeation enhancer, as reported in the literature for similar studies [71, 72]. Mechanistically, the solvation of lipophilic TE in SLNs rather than in water causes the concentration gradient towards the skin as observed for similar lipophilic drugs [73]. In addition, it is believed that nanoparticulate systems with small particle sizes have better chances to be in close contact with the stratum corneum (SC), thus, to adhere and penetrate into the skin to transport the drug in a controlled manner [74]. Furthermore, it is known that the SLNs exert an occlusive effect by forming films of dense-packed spheres on the surface of the skin, leading to increase skin hydration [71, 75]. These assumptions are consistent with those reported for similar studies. For example, Kelidari et al. explained that the spironolactone-SLNs exhibit a significant enhancement in the accumulative uptake of spironolactone through the skin onto the dispersion form of spironolactone [24]. Further, Guo et al. claimed that ivermectin-loaded SLNs formulations result in higher ivermectin penetration through the rat skin in comparison with the ivermectin suspension [31]. Finally, poor percutaneous absorption of the TE in the oleic acid oily solution can be related to the higher viscosity of this solution. These observations suggest that

suitable formulations of TE-SLNs would be regarded as the potential and efficient carriers for topical application of testosterone enanthate.

4. CONCLUSION

The present study successfully incorporated testosterone enanthate, which is a lipophilic drug, into a mixture of beeswax and surfactants to create a testosterone enanthate loaded solid lipid nanoparticles for transdermal delivery. The solid-state analysis of TE-SLNs indicated that testosterone enanthate dispersed into the lipid matrix in an amorphous form without any chemical interaction with average particle size, polydispersity index, zeta potential and encapsulation efficiency of 87.66± 1.52 nm, 0.317± 0.006, -23.06± 0.50 mV and 44.71± 1.14 %, respectively. In addition, in this examination, every significant visual change such as sedimentation, creaming and coalescence properties, as well as every alternation in the polydispersity index, particle size, zeta potential, and encapsulation efficiency for 90 days was recorded. According to the results, no considerable difference was observed. Furthermore, *in vitro* cytotoxicity study exhibited that the optimized testosterone enanthate loaded solid lipid nanoparticles have not been toxic due to an increased percentage of cell viability up to 100 %. Thus, this approach can be considered as a suitable alternative for the transdermal delivery of testosterone enanthate. Finally, it has been concluded that solid lipid nanoparticles are not only a promising carrier for topical delivery of testosterone enanthate, but also they could be applied as a carrier for the drugs that could cause gastrointestinal problems.

Conflict of interest

All authors claim no conflict of interest.

References

[1] A.A. Berthold, Transplantation der hoden, Arch Anat Physiol, (1849) 42-46.
[2] I. Alberti, A. Grenier, H. Kraus, D.N. Carrara, Pharmaceutical development and clinical effectiveness of a novel gel technology for transdermal drug delivery, Expert opinion on drug delivery, 2 (2005) 935-950.
[3] A.B. Champagne, K.V. Emmel, Rapid screening test for adulteration in raw materials of dietary supplements, Vibrational Spectroscopy, 55 (2011) 216-223.
[4] A. Vermeulen, Androgen replacement therapy in the aging male—a critical evaluation, The Journal of Clinical Endocrinology & Metabolism, 86 (2001) 2380-2390.
[5] M.P. Cramer, S.R. Saks, Translating safety, efficacy and compliance into economic value for controlled release dosage forms, Pharmacoeconomics, 5 (1994) 482-504.
[6] Y. Gu, M. Yang, X. Tang, T. Wang, D. Yang, G. Zhai, J. Liu, Lipid nanoparticles loading triptolide for transdermal delivery: mechanisms of penetration enhancement and transport properties, Journal of nanobiotechnology, 16 (2018) 68.
[7] H. Lee, C. Song, S. Baik, D. Kim, T. Hyeon, D.-H. Kim, Device-assisted transdermal drug delivery, Advanced drug delivery reviews, 127 (2018) 35-45.
[8] G.R. Cunningham, E. Cordero, J.I. Thornby, Testosterone replacement with transdermal therapeutic systems: physiological serum testosterone and elevated dihydrotestosterone levels, Jama, 261 (1989) 2525-2530.
[9] A.W. Meikle, N.A. Mazer, J.F. Moellmer, J.D. Stringham, K.G. Tolman, S.W. Sanders, W.D. Odell, Enhanced transdermal delivery of testosterone across nonscrotal skin produces physiological concentrations of testosterone and its metabolites in hypogonadal men, The Journal of Clinical Endocrinology & Metabolism, 74 (1992) 623-628.
[10] S. Parker, M. Armitage, Experience with transdermal testosterone replacement therapy for hypogonadal men, Clinical endocrinology, 50 (1999) 57-62.
[11] C. Carbone, E. Arena, V. Pepe, O. Prezzavento, I. Cacciatore, H. Turkez, A. Marrazzo, A. Di Stefano, G. Puglisi, Nanoencapsulation strategies for the delivery of novel bifunctional antioxidant/σ1 selective ligands, Colloids and Surfaces B: Biointerfaces, 155 (2017) 238-247.
[12] C. Tetyczka, M. Griesbacher, M. Absenger-Novak, E. Fröhlich, E. Roblegg, Development of nanostructured lipid carriers for intraoral delivery of domperidone, International journal of pharmaceutics, 526 (2017) 188-198.
[13] M. Nuruzzaman, M.M. Rahman, Y. Liu, R. Naidu, Nanoencapsulation, nano-guard for pesticides: a new window for safe application, Journal of agricultural and food chemistry, 64 (2016) 1447-1483.
[14] J. Pardeike, A. Hommoss, R.H. Müller, Lipid nanoparticles (SLN, NLC) in cosmetic and pharmaceutical dermal products, International journal of pharmaceutics, 366 (2009) 170-184.
[15] W. Mehnert, K. Mäder, Solid lipid nanoparticles: production, characterization and applications, Advanced drug delivery reviews, 64 (2012) 83-101.
[16] A. Lauterbach, C.C. Müller-Goymann, Applications and limitations of lipid nanoparticles in dermal and transdermal drug delivery via the follicular route, European Journal of Pharmaceutics and Biopharmaceutics, 97 (2015) 152-163.
[17] P. G Kakadia, B. R Conway, Lipid nanoparticles for dermal drug delivery, Current pharmaceutical design, 21 (2015) 2823-2829.
[18] M. Gupta, S.P. Vyas, Development, characterization and in vivo assessment of effective lipidic nanoparticles for dermal delivery of fluconazole against cutaneous candidiasis, Chemistry and physics of lipids, 165 (2012) 454-461.
[19] J. Liu, W. Hu, H. Chen, Q. Ni, H. Xu, X. Yang, Isotretinoin-loaded solid lipid nanoparticles with skin targeting for topical delivery, International journal of pharmaceutics, 328 (2007) 191-195.

[20] Q. Lv, A. Yu, Y. Xi, H. Li, Z. Song, J. Cui, F. Cao, G. Zhai, Development and evaluation of penciclovir-loaded solid lipid nanoparticles for topical delivery, International journal of pharmaceutics, 372 (2009) 191-198.
[21] M. Pradhan, D. Singh, M.R. Singh, Development characterization and skin permeating potential of lipid based novel delivery system for topical treatment of psoriasis, Chemistry and physics of lipids, 186 (2015) 9-16.
[22] A. Bhalerao, P.P. Chaudhari, Formulation of Solid Lipid Nanoparticles of Cilnidipine for the Treatment of Hypertension, Journal of Drug Delivery and Therapeutics, 9 (2019) 212-221.
[23] B.-J. Lin, W.-H. Chen, W.M. Budzianowski, C.-T. Hsieh, P.-H. Lin, Emulsification analysis of bio-oil and diesel under various combinations of emulsifiers, Applied energy, 178 (2016) 746-757.
[24] H. Kelidari, M. Saeedi, J. Akbari, K. Morteza-Semnani, P. Gill, H. Valizadeh, A. Nokhodchi, Formulation optimization and in vitro skin penetration of spironolactone loaded solid lipid nanoparticles, Colloids and Surfaces B: Biointerfaces, 128 (2015) 473-479.
[25] K. Oehlke, D. Behsnilian, E. Mayer-Miebach, P.G. Weidler, R. Greiner, Edible solid lipid nanoparticles (SLN) as carrier system for antioxidants of different lipophilicity, PloS one, 12 (2017) e0171662.
[26] J. Akbari, M. Saeedi, K. Morteza-Semnani, S.S. Rostamkalaei, M. Asadi, K. Asare-Addo, A. Nokhodchi, The design of naproxen solid lipid nanoparticles to target skin layers, Colloids and Surfaces B: Biointerfaces, 145 (2016) 626-633.
[27] B. Rodenak-Kladniew, G.A. Islan, M.G. de Bravo, N. Durán, G.R. Castro, Design, characterization and in vitro evaluation of linalool-loaded solid lipid nanoparticles as potent tool in cancer therapy, Colloids and Surfaces B: Biointerfaces, 154 (2017) 123-132.
[28] I.H.T. Guideline, Validation of analytical procedures: text and methodology Q2 (R1), International conference on harmonization, Geneva, Switzerland, 2005, pp. 11-12.
[29] R.B. Rigon, N. Fachinetti, P. Severino, A. Durazzo, M. Lucarini, A.G. Atanasov, S. El Mamouni, M. Chorilli, A. Santini, E.B. Souto, Quantification of Trans-Resveratrol-Loaded Solid Lipid Nanoparticles by a Validated Reverse-Phase HPLC Photodiode Array, Applied Sciences, 9 (2019) 4961.
[30] Q. Xu, T. Zhu, C. Yi, Q. Shen, Characterization and evaluation of metformin-loaded solid lipid nanoparticles for celluar and mitochondrial uptake, Drug development and industrial pharmacy, 42 (2016) 701-706.
[31] D. Guo, D. Dou, X. Li, Q. Zhang, Z.A. Bhutto, L. Wang, Ivermection-loaded solid lipid nanoparticles: preparation, characterisation, stability and transdermal behaviour, Artificial cells, nanomedicine, and biotechnology, 46 (2018) 255-262.
[32] L.L. Chaves, S. Lima, A.C. Vieira, D. Ferreira, B. Sarmento, S. Reis, Overcoming clofazimine intrinsic toxicity: statistical modelling and characterization of solid lipid nanoparticles, Journal of The Royal Society Interface, 15 (2018) 20170932.
[33] L. Tavano, P. Alfano, R. Muzzalupo, B. de Cindio, Niosomes vs microemulsions: new carriers for topical delivery of capsaicin, Colloids and surfaces B: Biointerfaces, 87 (2011) 333-339.
[34] T.J. Franz, Percutaneous absorption. On the relevance of in vitro data, Journal of Investigative Dermatology, 64 (1975) 190-195.
[35] P. Severino, S.C. Pinho, E.B. Souto, M.H. Santana, Polymorphism, crystallinity and hydrophilic–lipophilic balance of stearic acid and stearic acid–capric/caprylic triglyceride matrices for production of stable nanoparticles, Colloids and Surfaces B: Biointerfaces, 86 (2011) 125-130.
[36] A. Florence, J. Rogers, Emulsion stabilization by non-ionic surfactants: experiment and theory, Journal of Pharmacy and Pharmacology, 23 (1971) 233-251.
[37] D.A. Riehm, D.J. Rokke, P.G. Paul, H.S. Lee, B.S. Vizanko, A.V. McCormick, Dispersion of oil into water using lecithin-Tween 80 blends: The role of spontaneous emulsification, Journal of colloid and interface science, 487 (2017) 52-59.

[38] F. Han, S. Li, R. Yin, H. Liu, L. Xu, Effect of surfactants on the formation and characterization of a new type of colloidal drug delivery system: nanostructured lipid carriers, Colloids and Surfaces A: Physicochemical and Engineering Aspects, 315 (2008) 210-216.
[39] S. Kheradmandnia, E. Vasheghani-Farahani, M. Nosrati, F. Atyabi, Preparation and characterization of ketoprofen-loaded solid lipid nanoparticles made from beeswax and carnauba wax, Nanomedicine: Nanotechnology, Biology and Medicine, 6 (2010) 753-759.
[40] D. Chiaramonti, M. Bonini, E. Fratini, G. Tondi, K. Gartner, A. Bridgwater, H. Grimm, I. Soldaini, A. Webster, P. Baglioni, Development of emulsions from biomass pyrolysis liquid and diesel and their use in engines—Part 1: emulsion production, Biomass and bioenergy, 25 (2003) 85-99.
[41] W.C. Griffin, Calculation of HLB values of non-ionic surfactants, J. Soc. Cosmet. Chem., 5 (1954) 249-256.
[42] T. Schmidts, D. Dobler, A.-C. Guldan, N. Paulus, F. Runkel, Multiple W/O/W emulsions—Using the required HLB for emulsifier evaluation, Colloids and Surfaces A: Physicochemical and Engineering Aspects, 372 (2010) 48-54.
[43] D. Lu, D.G. Rhodes, Mixed composition films of spans and tween 80 at the Air− water interface, Langmuir, 16 (2000) 8107-8112.
[44] P. Severino, S.C. Pinho, E.B. Souto, M.H. Santana, Crystallinity of Dynasan® 114 and Dynasan® 118 matrices for the production of stable Miglyol®-loaded nanoparticles, Journal of thermal analysis and calorimetry, 108 (2011) 101-108.
[45] F.X. Gu, R. Karnik, A.Z. Wang, F. Alexis, E. Levy-Nissenbaum, S. Hong, R.S. Langer, O.C. Farokhzad, Targeted nanoparticles for cancer therapy, Nano today, 2 (2007) 14-21.
[46] K. Kato, P. Walde, N. Koine, S. Ichikawa, T. Ishikawa, R. Nagahama, T. Ishihara, T. Tsujii, M. Shudou, Y. Omokawa, Temperature-sensitive nonionic vesicles prepared from Span 80 (sorbitan monooleate), Langmuir, 24 (2008) 10762-10770.
[47] K. Kato, P. Walde, N. Koine, Y. Imai, K. Akiyama, T. Sugahara, Molecular Composition of Nonionic Vesicles Prepared from Span 80 or Span 85 by a Two-Step Emulsification Method, Journal of dispersion science and technology, 27 (2006) 1217-1222.
[48] I.D. de Souza, V. Saez, V.E. de Campos, C.R. Mansur, Size and Vitamin E Release of Nanostructured Lipid Carriers with Different Liquid Lipids, Surfactants and Preparation Methods, Macromolecular Symposia, Wiley Online Library, 2019, pp. 1800011.
[49] J.S. Negi, Nanolipid Materials for Drug Delivery Systems: A Comprehensive Review, Characterization and Biology of Nanomaterials for Drug Delivery, Elsevier2019, pp. 137-163.
[50] S. Lamaallam, H. Bataller, C. Dicharry, J. Lachaise, Formation and stability of miniemulsions produced by dispersion of water/oil/surfactants concentrates in a large amount of water, Colloids and Surfaces A: Physicochemical and Engineering Aspects, 270 (2005) 44-51.
[51] L. Wang, C.-Y. Wang, Y. Zhang, H.-J. Fu, Y. Gao, K.-R. Zhang, Preparation and characterization of solid lipid nanoparticles loaded with salmon calcitonin phospholipid complex, Journal of Drug Delivery Science and Technology, (2019).
[52] G. Abdelbary, R.H. Fahmy, Diazepam-loaded solid lipid nanoparticles: design and characterization, Aaps Pharmscitech, 10 (2009) 211-219.
[53] V. Venkateswarlu, K. Manjunath, Preparation, characterization and in vitro release kinetics of clozapine solid lipid nanoparticles, Journal of controlled release, 95 (2004) 627-638.
[54] A.A. Attama, C.C. Müller-Goymann, Effect of beeswax modification on the lipid matrix and solid lipid nanoparticle crystallinity, Colloids and Surfaces A: Physicochemical and Engineering Aspects, 315 (2008) 189-195.
[55] W. Luo, T. Li, C. Wang, F. Huang, Discovery of Beeswax as binding agent on a 6th-century BC Chinese Turquoise-inlaid Bronze sword, Journal of Archaeological Science, 39 (2012) 1227-1237.

[56] A. Farooq, H. Shafaghat, J. Jae, S.-C. Jung, Y.-K. Park, Enhanced stability of bio-oil and diesel fuel emulsion using Span 80 and Tween 60 emulsifiers, Journal of environmental management, 231 (2019) 694-700.
[57] J. Xiong, S. Xiong, Z. Guo, M. Yang, J. Chen, H. Fan, Ultrasonic dispersion of nano TiC powders aided by Tween 80 addition, Ceramics International, 38 (2012) 1815-1821.
[58] J. Hugel, The Identification of Testosterone and Eleven of its Esters, Canadian Society of Forensic Science Journal, 24 (1991) 147-164.
[59] G.A. Brewer, Gramicidin, Analytical Profiles of Drug Substances, Elsevier1979, pp. 179-218.
[60] W. Su, J. Darkwa, G. Kokogiannakis, Review of solid–liquid phase change materials and their encapsulation technologies, Renewable and Sustainable Energy Reviews, 48 (2015) 373-391.
[61] G.A. Islan, P.C. Tornello, G.A. Abraham, N. Duran, G.R. Castro, Smart lipid nanoparticles containing levofloxacin and DNase for lung delivery. Design and characterization, Colloids and Surfaces B: Biointerfaces, 143 (2016) 168-176.
[62] S.S. Montoto, M. Sbaraglini, A. Talevi, M. Couyoupetrou, M. Di Ianni, G. Pesce, V. Alvarez, L. Bruno-Blanch, G. Castro, M. Ruiz, Carbamazepine-loaded solid lipid nanoparticles and nanostructured lipid carriers: physicochemical characterization and in vitro/in vivo evaluation, Colloids and Surfaces B: Biointerfaces, 167 (2018) 73-81.
[63] M. Muchow, P. Maincent, R. Müller, C. Keck, Production and characterization of testosterone undecanoate-loaded NLC for oral bioavailability enhancement, Drug development and industrial pharmacy, 37 (2011) 8-14.
[64] K. Florey, Testosterone Enanthate, Analytical Profiles of Drug Substances, Elsevier1975, pp. 452-465.
[65] I. Basson, E. Reynhardt, An investigation of the structures and molecular dynamics of natural waxes. I. Beeswax, Journal of Physics D: Applied Physics, 21 (1988) 1421.
[66] N.M. Ranjha, H. Khan, S. Naseem, Encapsulation and characterization of controlled release flurbiprofen loaded microspheres using beeswax as an encapsulating agent, Journal of Materials Science: Materials in Medicine, 21 (2010) 1621-1630.
[67] S. Bhattacharjee, DLS and zeta potential–what they are and what they are not?, Journal of Controlled Release, 235 (2016) 337-351.
[68] R. Brydson, A. Brown, C. Hodges, P. Abellan, N. Hondow, Microscopy of nanoparticulate dispersions, Journal of microscopy, 260 (2015) 238-247.
[69] R.H. Müller, D. Rühl, S. Runge, K. Schulze-Forster, W. Mehnert, Cytotoxicity of solid lipid nanoparticles as a function of the lipid matrix and the surfactant, Pharmaceutical research, 14 (1997) 458-462.
[70] S. Talegaonkar, A. Bhattacharyya, Potential of lipid nanoparticles (SLNs and NLCs) in enhancing oral bioavailability of drugs with poor intestinal permeability, AAPS PharmSciTech, 20 (2019) 121.
[71] H. Chen, X. Chang, D. Du, W. Liu, J. Liu, T. Weng, Y. Yang, H. Xu, X. Yang, Podophyllotoxin-loaded solid lipid nanoparticles for epidermal targeting, Journal of controlled release, 110 (2006) 296-306.
[72] R.H. Müller, M. Radtke, S.A. Wissing, Solid lipid nanoparticles (SLN) and nanostructured lipid carriers (NLC) in cosmetic and dermatological preparations, Advanced drug delivery reviews, 54 (2002) S131-S155.
[73] J.-Y. Fang, C.-L. Fang, C.-H. Liu, Y.-H. Su, Lipid nanoparticles as vehicles for topical psoralen delivery: solid lipid nanoparticles (SLN) versus nanostructured lipid carriers (NLC), European Journal of Pharmaceutics and Biopharmaceutics, 70 (2008) 633-640.
[74] A. Kogan, N. Garti, Microemulsions as transdermal drug delivery vehicles, Advances in colloid and interface science, 123 (2006) 369-385.

[75] R.H. Müller, K. MaÈder, S. Gohla, Solid lipid nanoparticles (SLN) for controlled drug delivery–a review of the state of the art, European journal of pharmaceutics and biopharmaceutics, 50 (2000) 161-177.

692

693 Table 1. Effect of HLB on particle size, polydispersity index, zeta potential and encapsulation efficiency
694 for various TE-SLNs formulations

Formulation No.	HLB	Drug (g)	Lipid (g)	Span 80 (g)	Tween 80 (g)	Particle size (nm)	PDI	Zeta potential (mV)	EE (%)
F1	7.8	0.5	1	0.66	0.33	450.66± 1.52	0.743± 0.021	-3.86± 0.80	unstable
F2	7.8	0.5	1	1.33	0.66	342.66± 0.57	0.649± 0.046	-10.83± 1.10	1.95± 0.36
F3	7.8	0.5	1	2.00	1	346.66± 0.57	0.630± 0.050	-10.2± 0.91	1.13± 0.46
F4	9.6	0.5	1	0.50	0.5	242.33± 3.05	0.732± 0.021	-8.16± 1.02	unstable
F5	9.6	0.5	1	1.00	1	114.00± 1.73	0.485± 0.004	-17.3± 0.57	14.35± 1.71
F6	9.6	0.5	1	1.50	1.5	112.33± 0.57	0.478± 0.006	-17.3± 1.15	12.40± 2.25
F7	11.4	0.5	1	0.33	0.66	176.66± 2.08	0.57± 0.028	-15.56± 1.25	unstable
F8	11.4	0.5	1	0.66	1.33	87.66± 1.52	0.317± 0.006	-23.06± 0.50	44.71± 1.14
F9	11.4	0.5	1	1.00	2	88.33± 0.57	0.321± 0.006	-22.3± 1.53	21.62± 4.07
F10	15	0.5	1	0.00	1	320.33± 1.15	0.618± 0.051	-10.63± 1.41	unstable
F11	15	0.5	1	0.00	2	124.33± 2.51	0.463± 0.008	-18.5± 2.3	19.17± 1.54
F12	15	0.5	1	0.00	3	127.33± 1.52	0.446± 0.013	-17.73± 2.11	13.36± 1.33

695 Results are given as mean ± SD (n = 3).
696
697
698
699
700
701
702
703
704
705
706
707
708
709

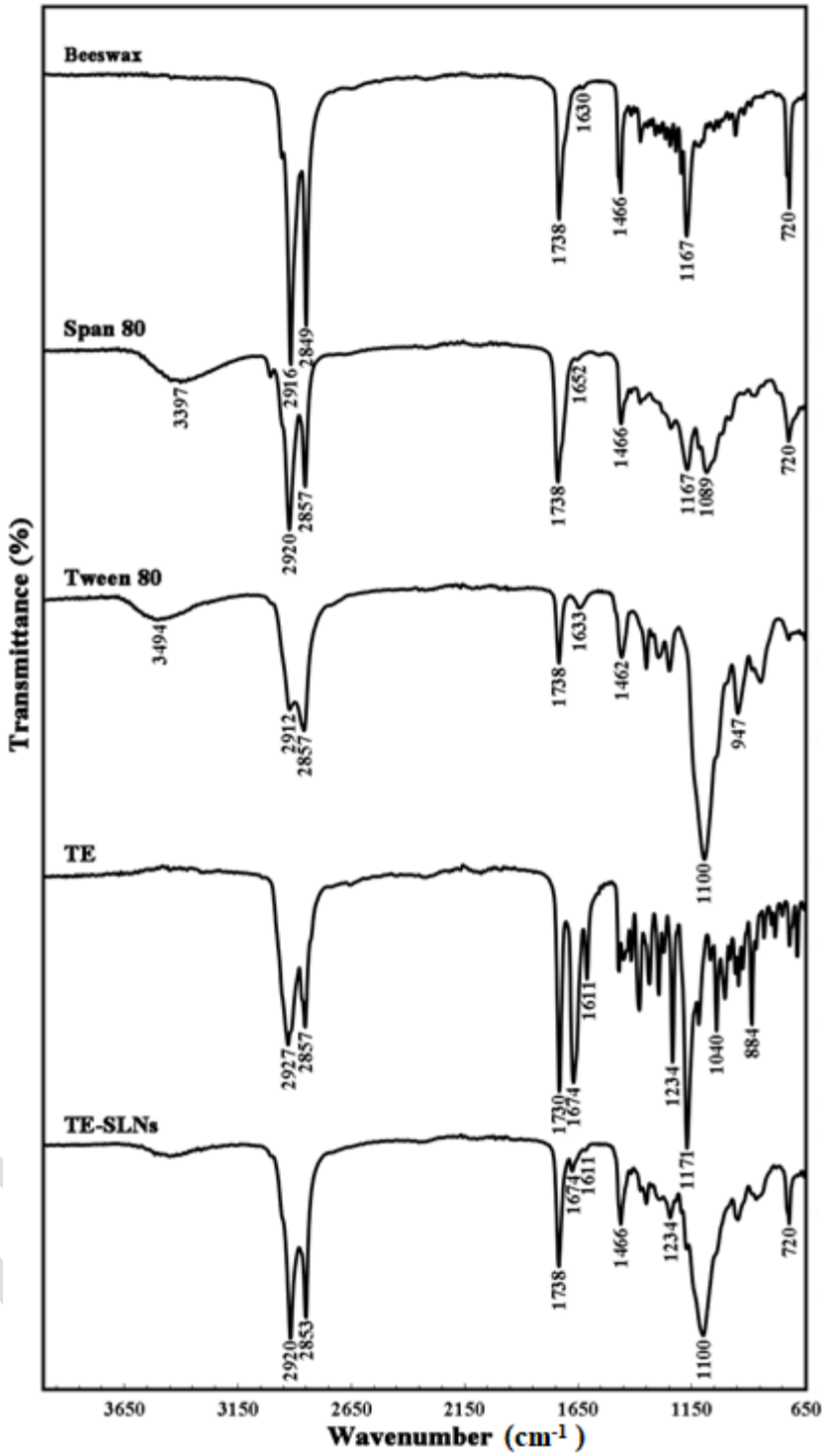

Fig 1. ATR-FTIR spectra of testosterone and excipients used in the preparation of nanoparticles including TE-SLN.

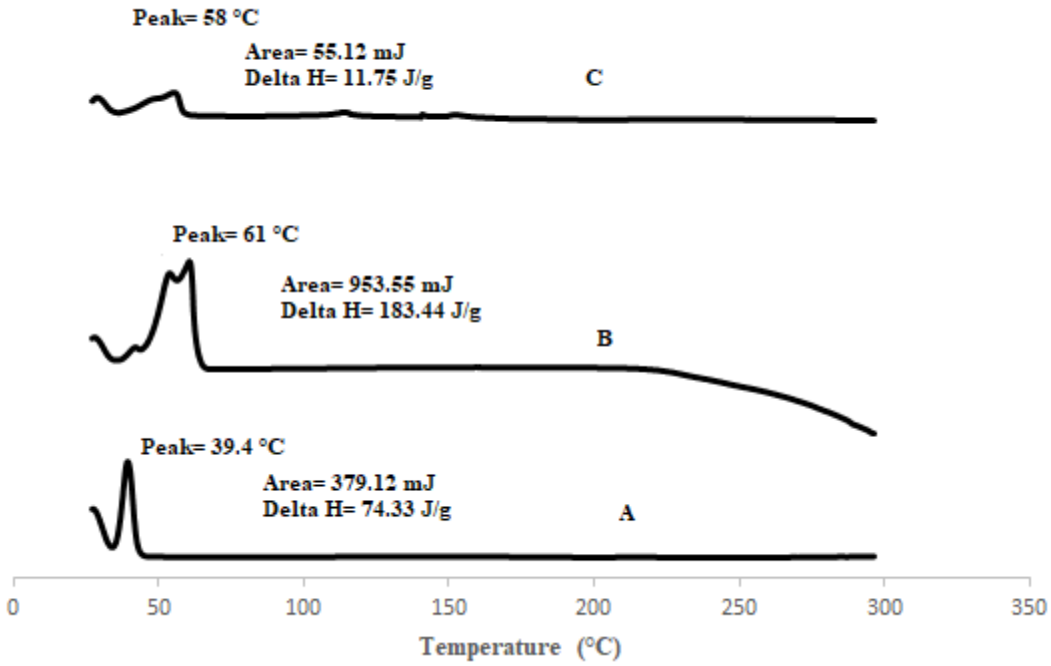

715

716 Fig 2. DSC curves of testosterone enanthate (A), beeswax (B) and TE-SLNs (C).

717

718

719

720

721

722

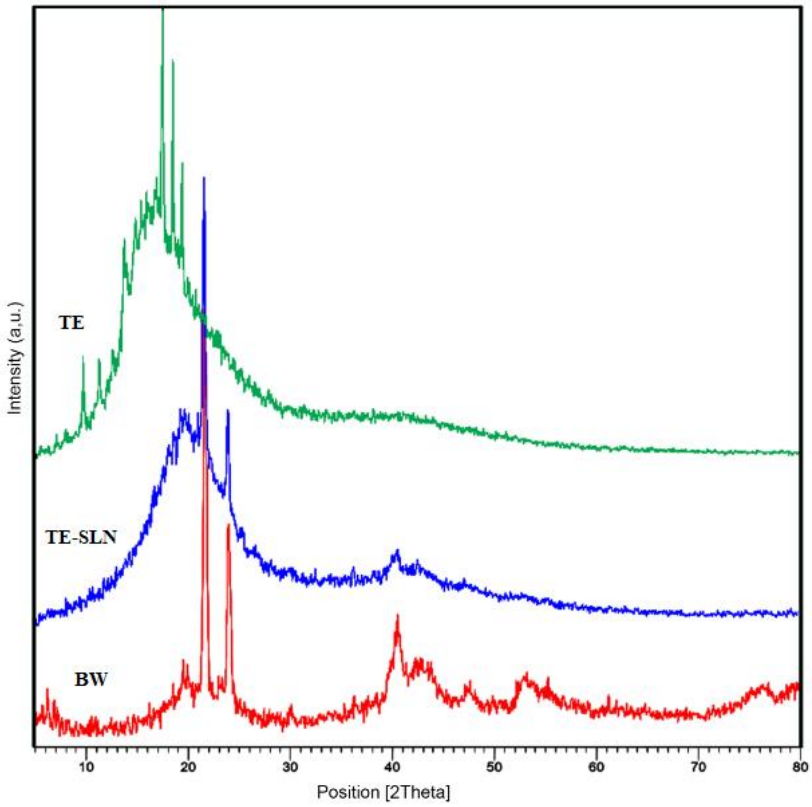

Fig. 3. XRD pattern of testosterone (TE), TE-SLN and beesewax (BW).

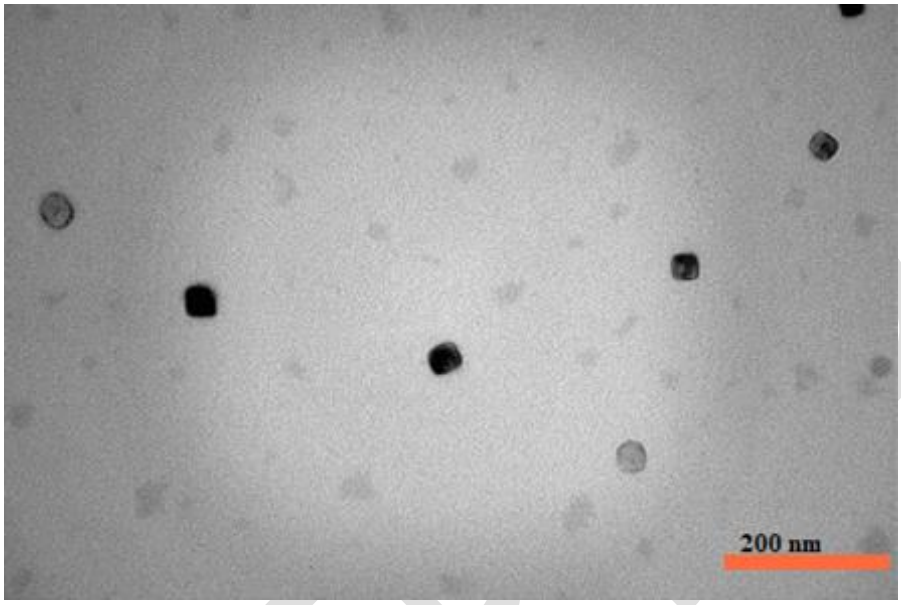

Fig 4.TEM image of TE-SLNs.

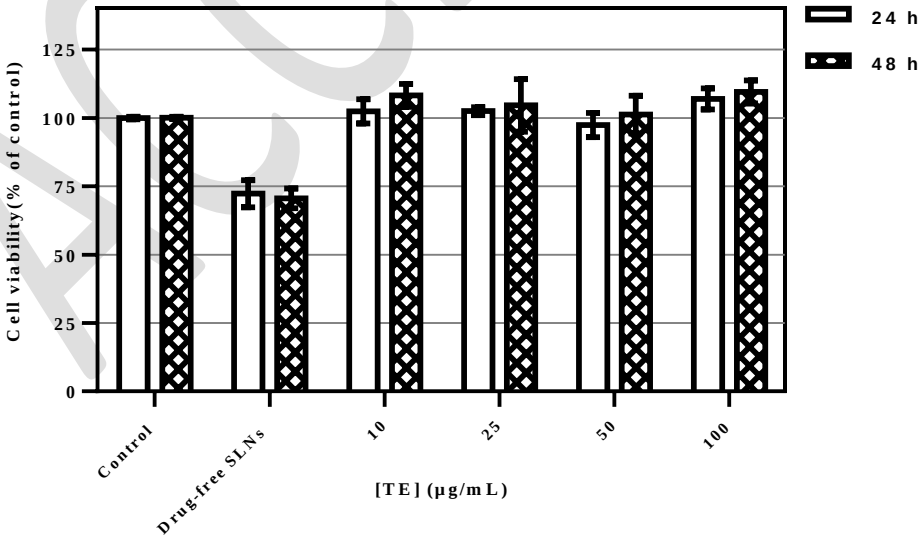

Fig 5. Cell viability of drug-free SLNs and different concentrations of TE-SLNs. Data are expressed as mean ± SD.

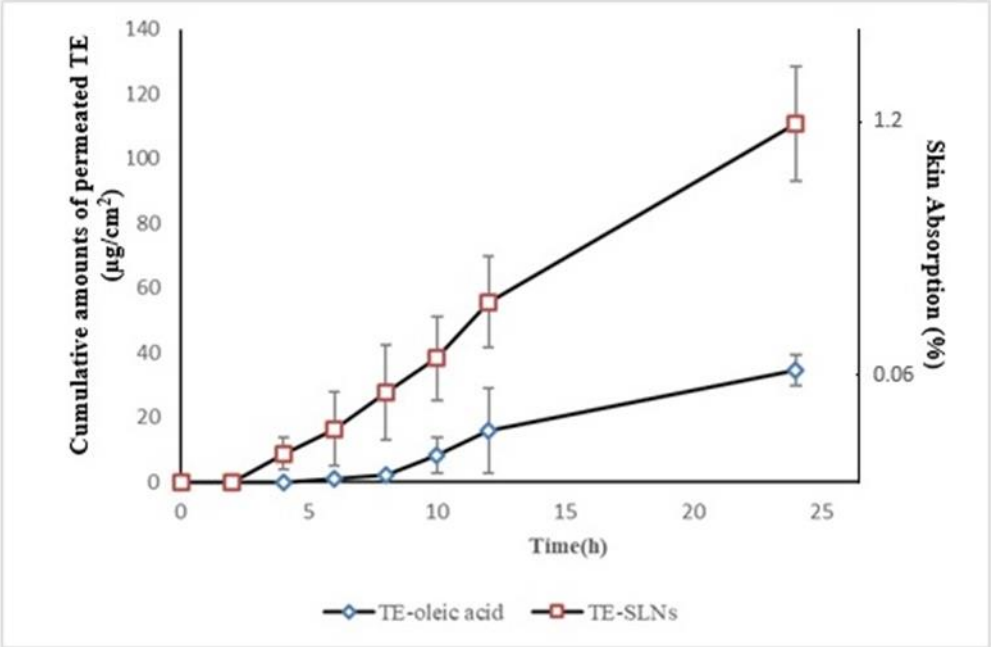

Fig 6. permeated TE from TE-oleic acid and TE-SLNs across rat skin. Data were expressed as the Mean ± SD.